



Retrogressed eclogite (20 kbar, 1020 °C) from the Neoproterozoic Palghat–Cauvery suture zone, southern India

K. Sajeev^{a,*}, B.F. Windley^b, J.A.D. Connolly^c, Y. Kon^d

^a Centre for Earth Sciences, Indian Institute of Science, Bangalore 560012, India

^b Department of Geology, University of Leicester, Leicester LE1 7RH, UK

^c Earth Sciences Department, Swiss Federal Institute of Technology, 8092 Zurich, Switzerland

^d Department of Earth and Planetary Sciences, Tokyo Institute of Technology, O-Okayama 2-12-1, Meguro, Tokyo 152-8551, Japan

ARTICLE INFO

Article history:

Received 7 October 2008

Received in revised form 18 February 2009

Accepted 1 March 2009

Keywords:

Retrogressed eclogite

Thermodynamic modeling

Hairpin-type anticlockwise *P–T* path

Subduction

Palghat–Cauvery suture zone

Southern India

ABSTRACT

The Palghat–Cauvery suture zone in southern India separates Archaean crustal blocks to the north and the Proterozoic Madurai block to the south. Here we present the first detailed study of a partially retrogressed eclogite (from within the Sittampundi anorthositic complex in the suture zone) that occurs as a 20-cm wide layer in a garnet gabbro layer in anorthosite. The eclogite largely consists of an assemblage of coexisting porphyroblasts of almandine–pyrope garnet and augitic clinopyroxene. However, a few garnets contain inclusions of omphacite. Rims and symplectites composed of Na–Ca amphibole and plagioclase form a retrograde assemblage. Petrographic analysis and calculated phase equilibria indicate that garnet–omphacite–rutile–melt was the peak metamorphic assemblage and that it formed at ca. 20 kbar and above 1000 °C. The eclogite was exhumed on a very tight hairpin-type, anticlockwise *P–T* path, which we relate to subduction and exhumation in the Palghat–Cauvery suture zone. The REE composition of the minerals suggests a basaltic oceanic crustal protolith metamorphosed in a subduction regime. Geological–structural relations combined with geophysical data from the Palghat–Cauvery suture zone suggest that the eclogite facies metamorphism was related to formation of the suture zone. Closure of the Mozambique Ocean led to development of the suture zone and to its western extension in the Betsimisaraka suture of Madagascar.

© 2009 Elsevier B.V. All rights reserved.

1. Introduction

The closure of the Mozambique Ocean in the Neoproterozoic led to the amalgamation of East and West Gondwana and the formation of the Mozambique suture (Fig. 1) (e.g., Meert, 2003; Collins, 2006; Meert and Lieberman, 2008; Rino et al., 2008). The Betsimisaraka suture in Madagascar (Collins and Windley, 2002) extends eastwards (present coordinates) across southern India most likely as the Palghat–Cauvery shear zone system—hereafter termed the Palghat–Cauvery suture zone (PCSZ) (Collins et al., 2007). Eclogites in the anorthositic Sittampundi complex were first described by Subramaniam (1956), but, perhaps because of the compositional caveat by Chappel and White (1970), it is surprising that eclogites were not reported from the PCSZ in ensuing decades. Recently Shimpo et al. (2006) reported high-pressure conditions within the MgO–Al₂O₃–SiO₂ chemical system from a nearby

garnet–corundum-bearing sapphirine granulite, but Kelsey et al. (2006) argued that the conclusions were unreliable. Thus the PCSZ has lacked well-defined, high-pressure eclogites, the presence of which would provide substantive confirmation of the former existence of a subduction zone.

Eclogite facies rocks worldwide occur in belts related to subduction–accretion and collisional tectonic settings (Maruyama et al., 1996). Later hydration and retrograde overprinting during exhumation commonly almost destroy the highest grade assemblages, and this can hamper tectonic interpretations. Following Subramaniam (1956), the second author (BFW) studied and sampled several eclogites in the Sittampundi complex in 1973, together with eclogites from other anorthositic–gabbroic complexes in the PCSZ. In the last year we returned to the Sittampundi complex twice to re-sample and confirm the occurrence of the eclogites. We have studied 65 polished sections of eclogites from our total collection, and found that just two have clear omphacite inclusions in garnet. We focus on sample M94 in this paper, because it has the best preserved and most definitive assemblage. This paper is one of the first reports of eclogite, albeit hydrated and partially retrogressed, in the Neoproterozoic suture zones of eastern Gondwana, and hence the discovery has implications for Gondwana tectonics.

* Corresponding author. Tel.: +91 80 2293 3404.

E-mail addresses: sajeev@ceas.iisc.ernet.in, krishnansajeew@gmail.com (K. Sajeev).

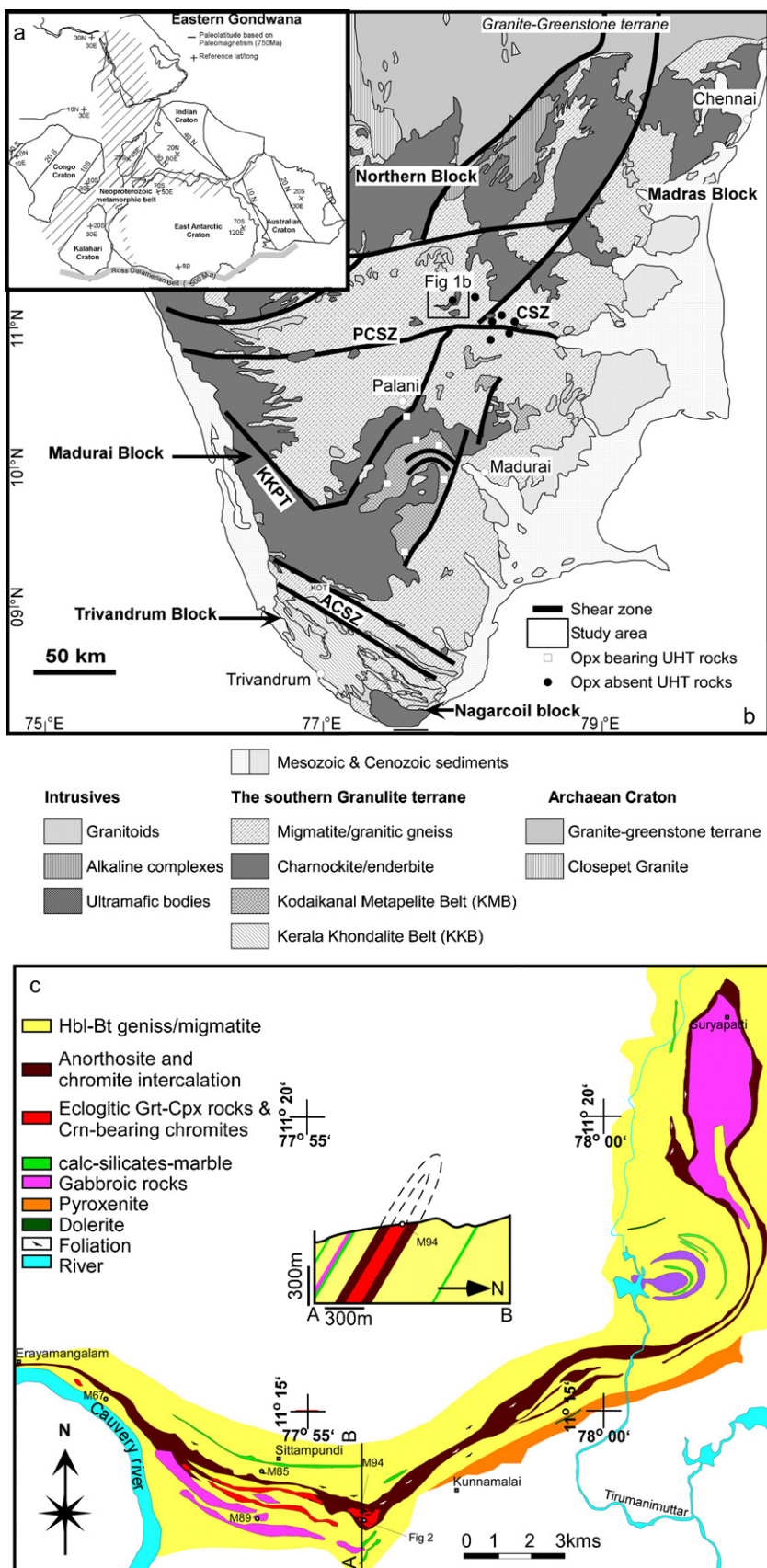


Fig. 1. (a) Paleogeographic reconstruction of eastern Gondwana (after Meert, 2003). (b) Simplified geological map of southern India (after Geological Survey of India, 1995; Ghosh et al., 2004; Santosh and Sajeev, 2006). (c) The geological map and sample locations of the Sittampundi complex (modified after Subramaniam, 1956; Ramadurai et al., 1975).

2. Geology of the Palghat–Cauvery suture zone

The Palghat–Cauvery suture zone refers to a series of major, largely EW-trending shear zones, Palghat, Cauvery, Moyar, Bhavani and Mettur (Fig. 1b) that cross southern India (Drury and Holt, 1980). This ca. 130-km wide suture zone marks a tectonic boundary between two continental blocks that have different isotopic characteristics, age, metamorphic, magmatic, structural and isotopic histories (e.g., Harris et al., 1994, 1996; Bartlett et al., 1998; Meißner et al., 2002; Bhaskar Rao et al., 2003; Ghosh et al., 2004). To the north are largely Archaean crustal blocks that contain granite–greenstone belts and granulites, and to the south is the largely Proterozoic Madurai block that includes the Southern Granulite Terrane (Fig. 1b). The Nilgiri Hills block is a major tectonic lens within the suture zone (Fig. 1b). The suture zone is characterized by the occurrence of many mafic–ultramafic complexes (Windley and Selvan, 1975; Bhaskar Rao et al., 1996; Chetty, 1996). Chetty and Bhaskar Rao (2006) demonstrated that the major shear zone network across the whole Palghat–Cauvery suture zone (Fig. 1b) defines a crustal-scale flower structure that formed as a result of dextral transpression interpreted to be a result of oblique collision between the Dharwar craton and the Madurai block.

The Palghat–Cauvery suture zone contains amphibolite facies migmatitic hornblende gneiss, hornblende–biotite gneiss, granitic orthogneiss, granulite facies orthopyroxene gneiss and massive charnockite (orthopyroxene–granite), which contain lenses of meta-sedimentary rocks such as paragneiss, meta-pelite, marble, calc–silicate rocks, and quartzite (e.g., Chetty, 1996). The Sittampundi area contains the km-scale mafic–ultramafic–anorthositic Sittampundi layered igneous complex, as well as layers of amphibolite with or without garnet, corundum or clinopyroxene, and useful, but rare, garnet–corundum–gedrite–Mg staurolite–sapphirine ultrahigh-temperature (990–940 °C at >12 kbar) granulites (e.g., Santosh et al., 2004; Shimpo et al., 2006; Santosh and Sajeev, 2006), and hōgbomite–spinel–sapphirine Mg–Al rocks (Tsunogae and Santosh, 2005). The Sittampundi complex (Subramaniam, 1956; Windley and Selvan, 1975; Windley et al., 1981) is a metamorphosed anorthositic complex about 36 km long and 2 km thick (maximum) with an original igneous stratigraphy overprinted by high-grade metamorphic assemblages (Fig. 1c) (Ramadurai et al., 1975). The complete stratigraphy from top to bottom is (with maximum thicknesses): clinozoisite anorthosite (ca. 150 m), hornblende anorthosite (ca. 75 m) with several chromitite seams (ca. 6 m), and amphibolitic meta-gabbro (ca. 750 m) that contains layers of pyroxenite up to 100 m long and lenses of eclogite a few

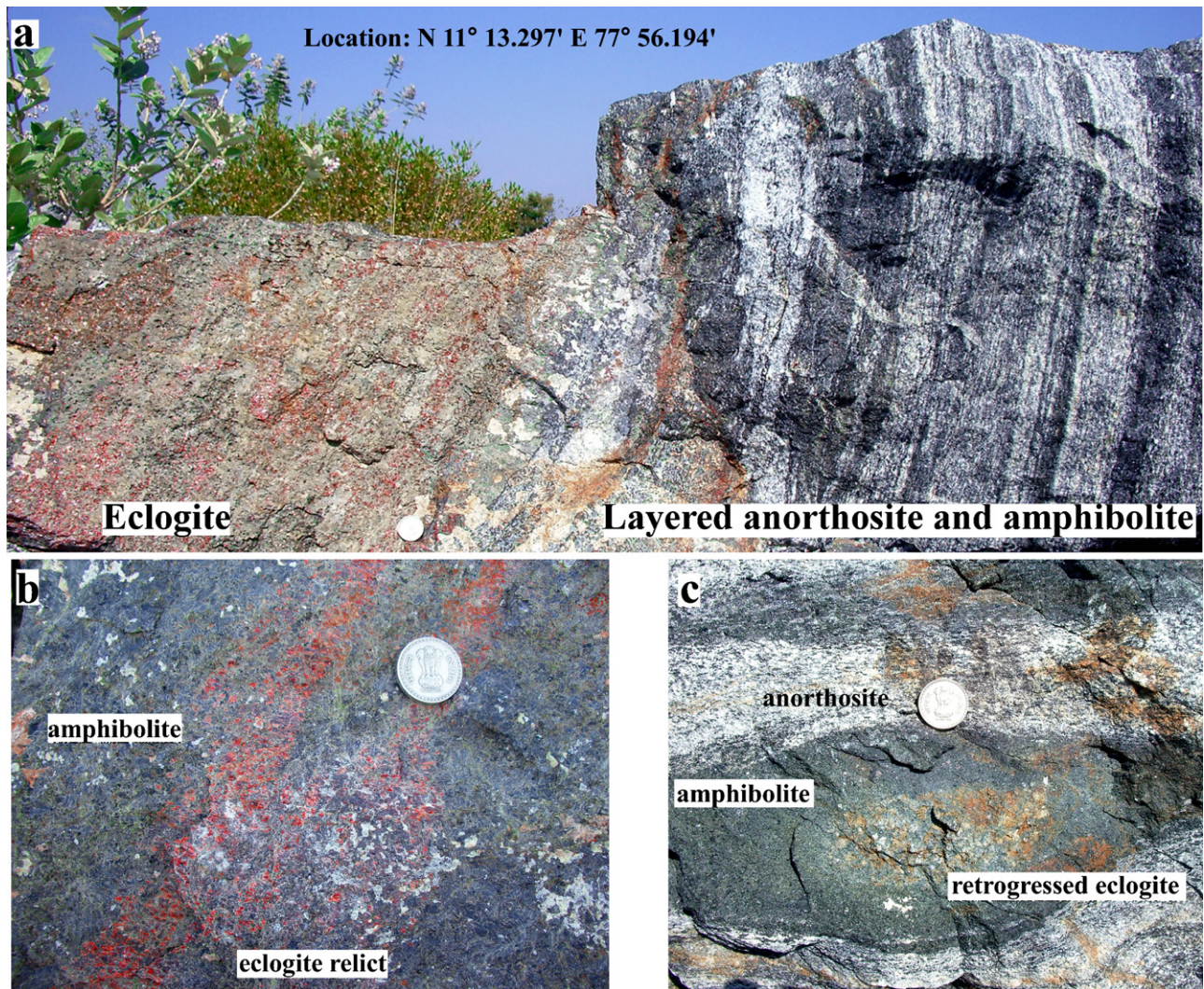


Fig. 2. New eclogite occurrences from a deep excavation site for a water tank (Fig. 2a gives the GPS location), less than 1 km south of the original 1973 locality (M94). (a) Large block of eclogite associated with inter-layered hornblende anorthosite and amphibolite. (b) A close-up view of eclogite that occurs as relict layers and lenses in garnet amphibolite. (c) Retrogressed eclogite preserved within the core of a garnet amphibolite layer within hornblende anorthosite. 2-cm wide coin for scale in a–c.

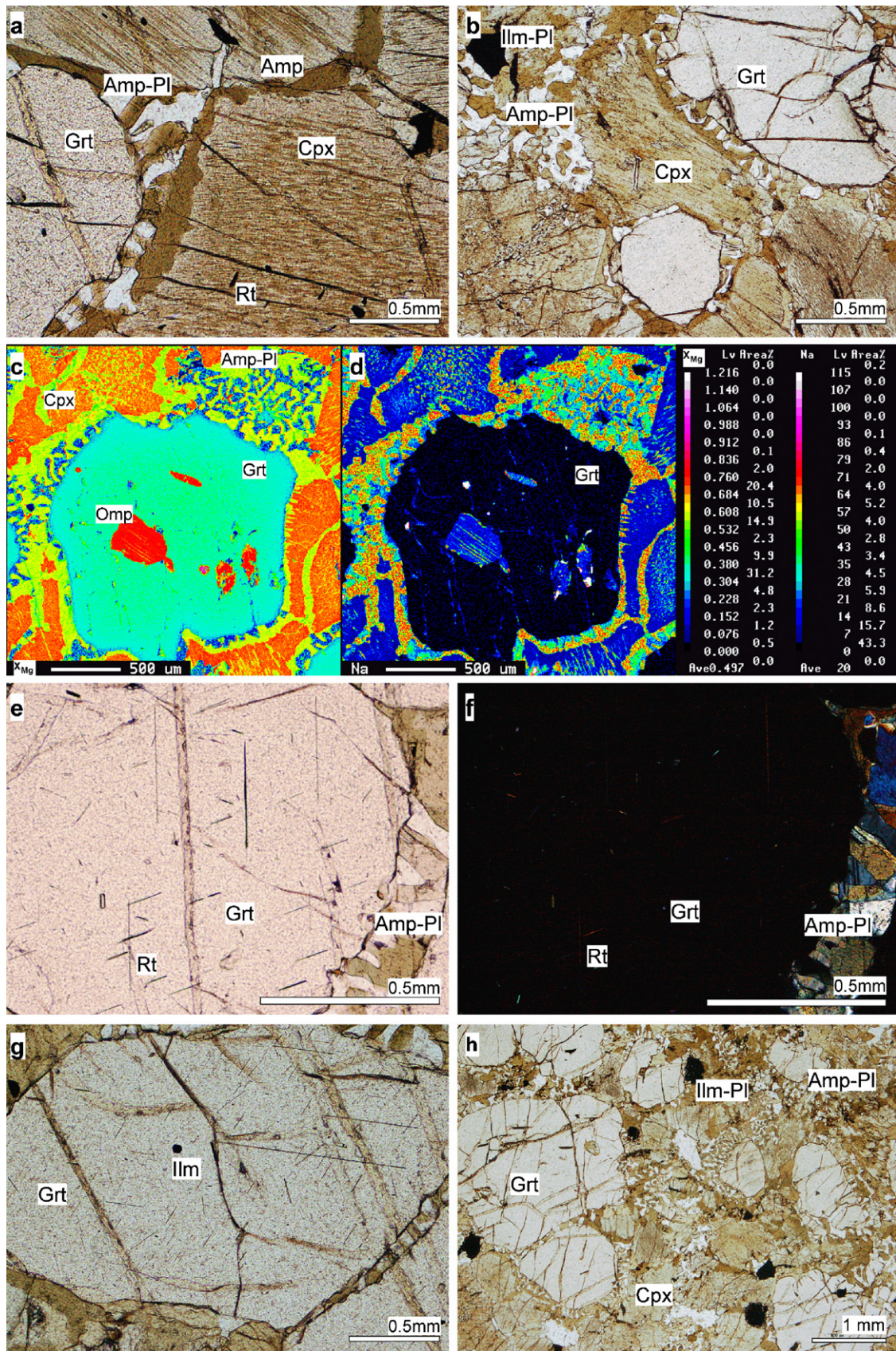


Fig. 3. Photomicrographs showing textural relations in retrogressed eclogites from the Sittampundi complex. (a) Major mineral assemblage of garnet and clinopyroxene porphyroblasts from eclogite sample M97. Note the rutile needles in garnet and clinopyroxene. The grain contacts between garnet and clinopyroxene are separated by late amphibole–plagioclase symplectite. (b) Partially retrogressed matrix of amphibole–ilmenite–plagioclase around resorbed garnet and clinopyroxene. (c) X-ray chemical mapping of garnet showing variations in X_{Mg} . (d) X-ray chemical mapping of garnet showing variations in Na content. Note the inclusion of omphacite in garnet and Na-rich amphibole separating garnet and clinopyroxene porphyroblasts. (e) Rutile exsolution lamellae within a garnet porphyroblast. (f) Crossed polar image of a garnet porphyroblast

metres long. As a result of isoclinal anticlinal folding, this stratigraphy is repeated in reverse order to give the present maximum thickness of about 2 km. Although there is tectonically modified igneous layering, no grading has been seen. The igneous upward stratigraphic direction referred to here is based on the assumption that the mafic-ultramafic rocks are at the bottom and the anorthosites are at the top. Thus the high-pressure eclogites are in the lowest level of the original stratigraphy, and occur in the present centre of the antiformally folded complex. Metamorphism of the Sittampundi complex has given rise to abundant clinzoisite in anorthosite, the eclogitic garnet–pyroxene rocks (Subramaniam, 1956; Chappel and White, 1970), anorthosites with assemblages of anorthite–clinzoisite–corundum–garnet ± hornblende and anorthite–garnet–vesuvianite (Subramaniam, 1956), garnet meta-gabbros, rocks containing hornblende, fuchsite, anthophyllite, diopside, sillimanite, Mg staurolite–sapphirine–kyanite (Ramadurai et al., 1975), gedrite, chrome spinel, and phlogopite (Janardhanan and Leake, 1974), two pyroxene pyroxenites, garnet–two pyroxene–hornblende rocks (Janardhanan and Leake, 1975), and high-pressure garnet–kyanite granulites (Collins et al., 2007). Chappel and White (1970), Janardhanan and Leake (1974, 1975), Ramadurai et al. (1975), Leake et al. (1976), and Bhaskar Rao et al. (2003) provided further data on the petrography, structure, stratigraphy, geochemistry and isotopic signature of the complex. Subramaniam (1956) first reported eclogitic garnet–clinopyroxene assemblages with analysed pyralmandites, and Chappel and White (1970) described other garnet–clinopyroxene assemblages that did not have eclogitic mineralogy. Nishimiya et al. (2008) also reported a nearby garnet–clinopyroxene rock (at Paramathi). Shimpoo et al. (2006) reported a magnesian staurolite-bearing, possible high-pressure, assemblage in pelitic granulite from a locality 5 km to the SE of the Sittampundi complex within the PCSZ. Garnet-absent and garnet-present sapphirine–gedrite granulites in surrounding areas in the PCSZ define a tight ‘hairpin-type’ anticlockwise *P–T* path at ultrahigh-temperature conditions (Santosh and Sajeev, 2006); this is one of the indications of a collision-type metamorphic belt (e.g., Maruyama and Okamoto, 2007).

The Sittampundi complex has been folded into an isoclinal antiform and refolded by an open fold with a N–S axial trace (Fig. 1c) (Ramadurai et al., 1975). Eclogites and retrogressed eclogites occur as layers and lenses up to 30–50-cm wide in anorthosite with interlayers of amphibolite (Fig. 2a), and as relicts in garnet amphibolite (Fig. 2b) layers in anorthosite (Fig. 2c). The retrogressed eclogite (sample M94) occurs as a 20-cm wide lensoid layer in a 150-m wide garnet meta-gabbro layer in anorthosite near the core of the isoclinal antiform. We ascribe the preservation of these high-pressure assemblages to their occurrence in the centre of the anorthosite complex that acted as a resistant bulwark to hydrous fluid infiltration, in contrast to the surrounding quartzo–feldspathic gneisses.

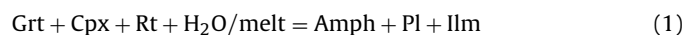
Co-magmatic rocks of the Sittampundi complex have a whole-rock Sm–Nd isochron age of $ca. 2935 \pm 60$ Ma interpreted as the time of a first metamorphism soon after emplacement; a second high-pressure metamorphism at $ca. 11.8$ kbar and 830°C (minimum) was inferred to have taken place at 726 ± 9 Ma based on a whole-rock garnet–plagioclase–hornblende Sm–Nd isochron age of a garnet granulite in the Sittampundi complex (Bhaskar Rao et al., 1996). The ultrahigh-temperature granulites in the PCSZ have a U–Pb zircon metamorphic age of 530 ± 4.9 Ma, monazite dates range from $ca. 525$ to 537 Ma, and inheritance ages are in the range of 2400–2600 Ma (Collins et al., 2007). High-grade rocks a

few kilometres NE of Sittampundi have Rb–Sr metamorphic ages of 700–800 Ma, and the Cauvery shear zone underwent isothermal decompression of 4.5–3.5 kbar followed by high-temperature hydration and retrogression at $ca. 600^\circ\text{C}$ (Bhaskar Rao et al., 1996). Shear zones along the suture zone have Sm–Nd garnet crystallization ages of 624–521 Ma and Rb–Sr biotite cooling/uplift ages of $ca. 600$ –480 Ma (Deters-Umlauf et al., 1998; Meißner et al., 2002; Ghosh et al., 2004). Finally, granulites within the PCSZ have a metamorphic zircon age of 535 ± 4.9 Ma and U–Th–Pb microprobe monazite ages in the range 550–520 Ma (Santosh et al., 2006) or 537–525 Ma (Collins et al., 2007); these ages, reflecting the time of ultrahigh-temperature metamorphism, were interpreted to constrain the age of the suture zone as latest Neoproterozoic to Cambrian. Seismic reflection and refraction studies constrained by gravity, magnetic and magnetotelluric data are consistent with the idea that the Palghat–Cauvery shear zone system marks a major suture zone between two contrasting tectonic blocks (Harinarayana et al., 2006; Rao and Prasad, 2006).

In summary, the Sittampundi complex was formed and underwent metamorphism in the Neoproterozoic, and was re-metamorphosed and re-deformed, together with other rocks in the suture zone in the Neoproterozoic–Cambrian, which we interpret as the time when it was incorporated into the suture zone and the deep continental crust.

3. Petrography of eclogite

The partially retrogressed eclogite (M94) from the Sittampundi complex has a major mineral assemblage of garnet + clinopyroxene porphyroblasts (Fig. 3a). The porphyroblast grain size varies from $ca. 5$ to 6 mm in diameter. The garnet and clinopyroxene porphyroblasts are commonly mantled by rims (of variable thickness) and symplectites of Ca–Na–amphibole and plagioclase (Fig. 3a, b); the latter also occur in places as separate grains in mutual contact. Plagioclase and amphibole only occur as retrograde phases, thus these eclogites definitely formed as plagioclase-free high-pressure rocks. Garnet cores contain inclusions of clinopyroxene (Fig. 3e, f), and minor garnet grains are observed within some clinopyroxenes. Most clinopyroxene porphyroblasts and most clinopyroxene inclusions within garnet are overprinted by a late growth of Ca–Na–amphibole along their grain boundaries and cleavages; only a few inclusions are preserved with no amphibole overprint (Fig. 3a–d). The granoblastic garnets contain needles and/or lamellae of rutile (Fig. 3g, h), which distinctively show inclined extinction. Rare rutile with inclined extinction was recorded in eclogites from kimberlites in South Africa by Griffin et al. (1971), who suggested it indicates the former presence of a titanium-rich garnet or a TiO₂ polymorph in a prograde or near-peak eclogitic stage of metamorphism. Our major retrograde assemblage is amphibole–plagioclase symplectite along the grain boundaries of garnet and clinopyroxene. Minor symplectites of late ilmenite–plagioclase have formed with amphibole-bearing assemblages in the retrograde matrix (Fig. 3h); these probably developed according to the following decompression reaction and hydration after peak metamorphism:



In amphibole-rich retrogressed domains there are relicts of fine-grained clinopyroxenes within a Ca–Na–amphibole matrix. Minor inclusions of ilmenite occur within garnet and clinopyroxene cores (Fig. 3g) probably representing a prograde phase. We have never seen orthopyroxene or spinel in any textural setting.

4. Major element mineral chemistry

Electron microprobe analyses of the eclogite were carried out using a JEOL JXA-8900R microprobe at the Okayama University of Science, operating with an accelerating voltage of 15 kV, and a beam current of 12 nA. Natural and synthetic silicates and oxides were used for calibration. The data were reduced using ZAF correction procedures. Representative mineral analyses are given in Tables 1 and 2.

4.1. Garnet

Garnet porphyroblasts are enriched in almandine and pyrope with lesser amounts of grossular (Prp_{40.9–30.2}, Alm_{46.5–38.1}, Grs_{25.8–18.3}). Chemical zonations from core to rim are rarely observed. Garnet inclusions within clinopyroxene have a composition similar to that of the porphyroblasts.

4.2. Clinopyroxene

The clinopyroxene porphyroblasts associated with garnet are mainly augite (Aug_{76.5–53.4}) with a minor jadeite component (Jd_{0.0–3.9}); X_{Mg} [Mg/(Fe²⁺ + Mg)] of the augite varies from 0.758 to 0.727. The clinopyroxenes inclusions within garnet with little/no amphibole along their cleavages have relatively high Na₂O contents (up to 4.56 wt% Jd_{21.0–13.6}), and accordingly they fall within the omphacite field indicating the presence of highly sodic clinopyroxene (omphacite) before hydration at peak eclogite facies conditions.

In summary, the garnets containing omphacitic inclusions acted as a bulwark protecting the inclusions from fluid ingress and hydration to amphibole, whereas the porphyroblastic clinopyroxenes were modified to augite by extensive fluid migration through the matrix. We consider that the augitic porphyroblasts with Na–Ca amphibole cleavage overgrowths originally formed as a peak assemblage, similar to that of the inclusions, but their compositions were changed during hydration.

4.3. Retrograde minerals (amphibole and plagioclase)

Amphiboles in retrograde rims and symplectites are enriched in calcium and sodium (Ca + Na = ca. 2.0) with X_{Mg} varying from 0.682 to 0.650; they resulted from the breakdown of clinopyroxene in the presence of garnet. Retrograde plagioclases associated with amphibole are slightly enriched in albite (Ab_{54.2–48.2}, An_{51.5–45.5}); they compliment the breakdown of Na-rich clinopyroxene with garnet.

In conclusion, the presence of omphacite in garnet porphyroblasts and the later Ca–Na–amphibole and plagioclase replacement (mainly of the jadeitic component) of clinopyroxene porphyroblasts indicate hydration of the rocks after they reached near-peak eclogite facies conditions. Such Ca–Na–amphibole replacement can be interpreted as the result of breakdown and hydration during decompression through reaction (1) above. It is also important to note that low-pressure granulite facies minerals like orthopyroxene are completely absent in our samples. Exsolution of rutile could have developed from a Ti-rich garnet at the near-peak or just after the peak eclogite-facies metamorphism. Minor ilmenite inclusions in garnet and clinopyroxene possibly represent an earlier stage (prograde) before the attainment of eclogite facies conditions. Some eclogitic samples are so completely overprinted by amphiboles that only minor clinopyroxenes are preserved within garnet cores. Based on petrographic observations and mineral assemblages we conclude that the best preserved rocks had an assemblage of garnet–omphacite ± rutile that was stable under eclogite facies conditions, that the only preserved prograde phase is ilmenite, and that the peak assemblage was later overprinted by Ca–Na–amphibole and plagioclase. Clinopyroxene porphyroblasts

are texturally associated with the peak metamorphic assemblage, but their bulk chemical composition was changed by fluids during the retrograde overprint.

5. Rare earth element composition of minerals

Rare earth element (REE) compositions of garnet, omphacite, clinopyroxene, amphibole and plagioclase were determined by laser ablation–inductively coupled plasma mass spectrometry (LA–ICPMS) at the Tokyo Institute of Technology, Japan. The analytical procedures strictly followed the method outlined by [Iizuka and Hiratha \(2004\)](#). The REE concentrations of the major phases are presented in Tables 3 and 4. All the analyses were carried out with a 16 μm laser beam diameter. In order to avoid problems caused by late metasomatism and diffusion extreme care was taken to fix the analytical points. All the analyses were carried out with time-resolved analysis of the ablation signals. The samples were later petrographically checked to avoid any analysis of retrograde assemblages, cracks and fractures. Any analyses with problems of analytical errors of contamination were excluded.

Garnet preserves high concentrations of heavy REE (HREE) and is depleted in light REE (LREE) with average C1 chondrite-normalized (Evensen et al., 1978) La (La_N) and Yb (Yb_N) values ranging from 0.04 to 0.25 and 36.42 to 21.61 respectively (Fig. 4a). Most garnets have a high HREE content (Yb from 6.01 to 3.57 parts per million; ppm) with a relatively flat profile ((Dy/Yb)_N = 1.29–1.67). The Sr content in garnet is very low (0.41–0.02 ppm) and sometimes below the detection limit. Omphacite occurring as inclusions in garnet has an opposite pattern to that of garnet being LREE-enriched relative to the HREE. La_N content ranges from 2.44 to 1.78, while Yb_N = 0.62–0.11 (Fig. 4b). HREE of garnet and LREE of

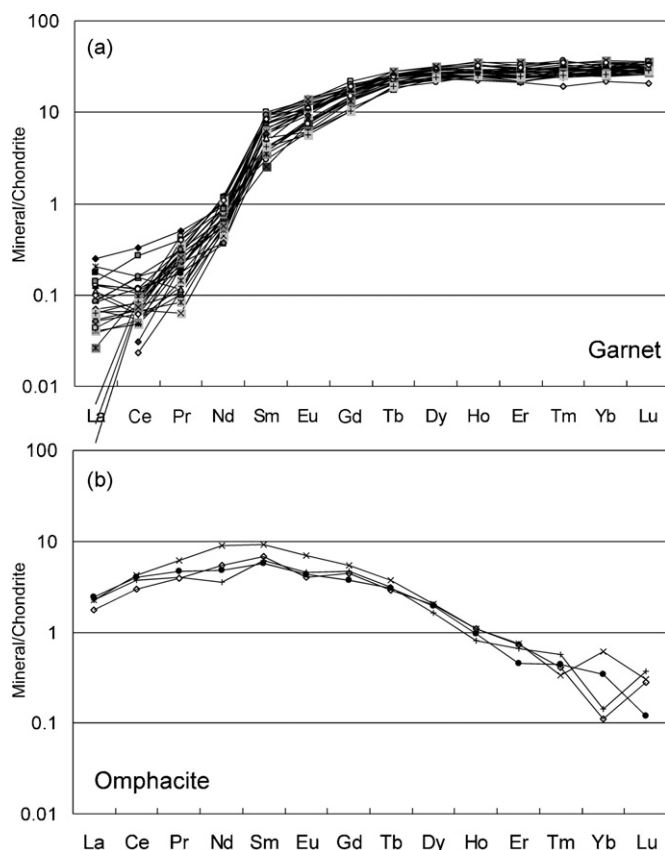


Fig. 4. C1 chondrite-normalized REE pattern of primary minerals. (a) garnet and (b) omphacite from Sittampundi eclogite. See text for further discussion.

Table 1
Representative mineral chemistry of garnet, omphacite and clinopyroxene from Sittampundi eclogite.

	Garnet						Omphacite						Clinopyroxene						
SiO ₂	40.41	40.04	40.06	39.52	40.07	39.50	53.89	53.02	53.53	53.87	53.41	53.16	53.23	52.07	51.37	51.48	51.37	52.02	50.35
TiO ₂	0.03	0.05	0.05	0.03	0.04	0.06	0.20	0.00	0.00	0.30	0.37	0.08	0.00	0.52	0.55	0.49	0.59	0.35	0.90
Al ₂ O ₃	22.56	21.54	21.93	22.17	21.63	21.85	6.74	7.08	6.73	6.54	6.13	6.56	6.14	3.40	3.44	3.42	3.67	3.98	5.82
Cr ₂ O ₃	0.00	0.00	0.00	0.03	0.01	0.03	0.20	0.06	0.00	0.50	0.00	0.00	0.03	0.03	0.00	0.02	0.00	0.01	0.00
FeO	18.56	18.06	19.39	21.01	21.70	21.96	8.32	10.06	9.04	8.56	9.28	9.52	7.97	7.93	7.71	7.56	7.74	7.56	8.77
MnO	0.00	0.01	0.02	0.00	0.00	0.02	0.01	0.01	0.00	0.00	0.00	0.00	0.00	0.00	0.02	0.00	0.00	0.01	0.00
MgO	9.99	9.77	10.97	8.77	8.77	7.99	9.68	11.00	10.02	10.01	11.18	12.00	13.77	13.57	13.25	13.19	13.23	13.30	13.10
CaO	9.39	9.72	7.08	8.55	8.13	8.56	16.04	16.03	16.43	16.17	15.90	15.72	14.50	23.10	23.16	23.14	22.63	21.03	19.52
Na ₂ O	0.03	0.00	0.02	0.04	0.05	0.02	4.88	3.14	4.42	4.56	3.52	3.41	3.52	0.25	0.22	0.31	0.37	1.04	0.85
K ₂ O	0.00	0.00	0.00	0.00	0.01	0.01	0.00	0.00	0.00	0.01	0.02	0.00	0.00	0.00	0.00	0.00	0.02	0.00	0.01
Total	100.95	99.19	99.50	100.11	100.40	100.00	99.96	100.40	100.17	100.52	99.80	100.45	99.16	100.90	99.73	99.61	99.62	99.30	99.32
O	12						6						6						
Si	3.007	3.035	3.021	2.999	3.035	3.014	1.977	1.944	1.966	1.969	1.965	1.945	1.954	1.918	1.916	1.921	1.915	1.935	1.877
Ti	0.002	0.003	0.003	0.002	0.002	0.004	0.006	0.000	0.000	0.008	0.010	0.002	0.000	0.014	0.016	0.014	0.017	0.010	0.025
Al	1.979	1.924	1.949	1.983	1.931	1.966	0.291	0.306	0.291	0.282	0.266	0.283	0.266	0.148	0.151	0.150	0.161	0.174	0.256
Cr	0.000	0.000	0.000	0.001	0.001	0.002	0.006	0.002	0.000	0.014	0.000	0.000	0.001	0.001	0.000	0.001	0.000	0.000	0.000
Fe	1.155	1.145	1.223	1.333	1.375	1.402	0.255	0.308	0.278	0.262	0.286	0.291	0.245	0.244	0.240	0.236	0.241	0.235	0.273
Mn	0.000	0.001	0.001	0.000	0.000	0.001	0.000	0.000	0.000	0.000	0.000	0.000	0.000	0.000	0.001	0.000	0.000	0.000	0.000
Mg	1.108	1.103	1.233	0.991	0.989	0.908	0.529	0.601	0.548	0.545	0.613	0.654	0.753	0.745	0.736	0.733	0.735	0.737	0.728
Ca	0.749	0.789	0.572	0.695	0.660	0.700	0.631	0.630	0.647	0.633	0.627	0.616	0.570	0.912	0.926	0.925	0.904	0.838	0.780
Na	0.004	0.000	0.003	0.005	0.007	0.003	0.347	0.223	0.315	0.323	0.251	0.242	0.250	0.018	0.016	0.023	0.027	0.075	0.061
K	0.000	0.000	0.000	0.000	0.001	0.001	0.000	0.000	0.000	0.000	0.001	0.000	0.000	0.000	0.000	0.000	0.001	0.000	0.000
Total cation	8.004	8.000	8.004	8.010	8.001	8.001	4.042	4.014	4.045	4.037	4.018	4.033	4.038	4.002	4.001	4.002	4.001	4.006	4.001
X _{Mg}	0.49	0.49	0.50	0.43	0.42	0.39	0.67	0.66	0.66	0.68	0.68	0.69	0.76	0.75	0.75	0.76	0.75	0.76	0.73
Alm	0.381	0.377	0.402	0.435	0.454	0.465	Ac	0.126	0.043	0.134	0.109	0.053	0.097	0.114	0.006	0.004	0.005	0.004	0.002
Sps	0.000	0.000	0.000	0.000	0.000	0.000	Ca–Es	0.035	0.012	0.044	0.021	0.017	0.032	0.037	0.001	0.001	0.001	0.001	0.000
Prp	0.369	0.363	0.409	0.332	0.328	0.302	CaTs	0.023	0.056	0.034	0.031	0.035	0.055	0.046	0.082	0.084	0.079	0.085	0.123
Grs	0.243	0.257	0.183	0.217	0.215	0.230	Jd	0.210	0.181	0.180	0.197	0.178	0.140	0.136	0.000	0.000	0.000	0.000	0.009
							Aug	0.567	0.511	0.558	0.560	0.548	0.489	0.459	0.749	0.756	0.765	0.734	0.534
							Opx	0.043	0.178	0.067	0.064	0.144	0.178	0.212	0.111	0.101	0.093	0.111	0.220

Clinopyroxene endmembers calculated following the procedure of Katayama et al. (2002).

X_{Mg} = [Mg/(Fe + Mg)].

Prp = [Mg/(Mg + Fe + Mn + Ca)].

Alm = [Fe/(Mg + Fe + Mn + Ca)].

Grs = [Ca/(Mg + Fe + Mn + Ca)].

Sps = [Mn/(Mg + Fe + Mn + Ca)].

Table 2
Representative mineral chemistry of plagioclase and amphibole from Sittampundi eclogite.

Plagioclase in symplectite						Amphibole in symplectite					
SiO ₂	56.21	55.50	54.78	56.31	55.11	41.23	41.20	41.03	40.96	41.19	39.28
TiO ₂	0.08	0.00	0.00	0.07	0.62	2.64	2.74	3.42	3.46	3.35	3.36
Al ₂ O ₃	27.53	28.03	28.52	27.31	27.65	12.71	13.19	12.60	12.40	12.65	12.11
FeO	0.37	0.30	0.22	0.37	0.25	12.42	11.76	12.65	12.69	11.99	12.43
MnO	0.05	0.01	0.04	0.04	0.03	0.07	0.12	0.07	0.06	0.09	0.10
MgO	0.02	0.00	0.00	0.03	0.01	12.31	12.22	12.39	12.08	11.89	11.70
CaO	10.00	10.63	11.26	10.01	10.48	11.60	11.63	11.37	11.17	11.46	11.50
Na ₂ O	6.39	6.11	5.83	6.59	6.44	2.43	2.42	2.34	2.41	2.03	1.86
K ₂ O	0.07	0.06	0.05	0.04	0.09	0.89	0.96	1.40	1.35	1.35	1.34
H ₂ O*	–	–	–	–	–	2.01	2.01	2.02	2.00	1.99	1.94
Total	100.72	100.62	100.70	100.77	100.68	98.54	98.36	99.53	98.79	98.04	95.81
O	8		23								
Si	2.518	2.492	2.463	2.523	2.479	6.161	6.159	6.093	6.131	6.195	6.079
Ti	0.003	0.000	0.000	0.002	0.021	0.296	0.308	0.382	0.389	0.378	0.392
Al	1.454	1.483	1.511	1.442	1.466	–	–	–	–	–	–
Al iv	–	–	–	–	–	1.839	1.841	1.907	1.869	1.805	1.921
Al vi	–	–	–	–	–	0.399	0.483	0.297	0.319	0.436	0.287
Fe	0.014	0.011	0.008	0.014	0.009	–	–	–	–	–	–
Fe ³⁺	–	–	–	–	–	0.257	0.129	0.292	0.231	0.071	0.213
Fe ²⁺	–	–	–	–	–	1.295	1.341	1.279	1.357	1.437	1.396
Mn	0.002	0.000	0.002	0.002	0.001	0.009	0.016	0.008	0.007	0.011	0.014
Mg	0.001	0.000	0.000	0.002	0.001	2.743	2.723	2.742	2.696	2.666	2.699
Ca	0.480	0.511	0.542	0.481	0.505	1.858	1.863	1.809	1.792	1.846	1.907
Na	0.555	0.532	0.508	0.572	0.562	0.705	0.703	0.673	0.698	0.591	0.559
K	0.004	0.003	0.003	0.002	0.005	0.170	0.184	0.264	0.259	0.258	0.264
OH*	–	–	–	–	–	2.000	2.000	2.000	2.000	2.000	2.000
Total cation	5.031	5.034	5.037	5.041	5.050	17.732	17.750	17.746	17.749	17.696	17.730
An	0.462129	0.4886126	0.514824	0.4554644	0.4711496	Ca + Na	2	2	2	2	2
Ab	0.534129	0.5081578	0.4824531	0.5423685	0.5239258	Na + K	0.7323218	0.7498018	0.745949	0.7488093	0.6955276
Or	0.003742	0.0032296	0.0027229	0.002167	0.0049246	X _{Mg}	0.6792767	0.6700989	0.6819087	0.6652089	0.64971

Maximum estimate for Fe³⁺ in amphibole using the 13eCNK calculation after Robinson et al. (1982).

An = Ca/(Ca + Na + K).

Ab = Na/(Ca + Na + K).

Or = K/(Ca + Na + K).

X_{Mg} = Mg/(Mg + Fe²⁺).

Table 3
REE composition of garnet and omphacite determined by LA-ICPMS.

	Sr	Y	Zr	La	Ce	Pr	Nd	Sm	Eu	Gd	Tb	Dy	Ho	Er	Tm	Yb	Lu
Garnet																	
M94-1-01	0.18	40.26	9.47	bd	0.01	0.01	0.57	1.43	0.74	3.49	0.81	5.87	1.42	3.64	0.64	4.42	0.68
M94-1-02	bd	41.61	3.88	0.04	0.07	0.02	0.17	1.01	0.64	3.18	0.85	6.84	1.49	4.21	0.75	4.88	0.71
M94-1-03	bd	42.40	3.13	0.02	0.04	0.01	0.24	1.14	0.61	3.38	0.85	6.53	1.56	4.20	0.74	4.48	0.77
M94-1-04	0.06	45.34	2.60	0.01	0.04	0.01	0.21	0.95	0.60	3.36	0.96	6.93	1.63	4.58	0.71	4.82	0.73
M94-1-05	0.21	45.18	2.78	0.02	0.04	0.01	0.25	0.93	0.58	3.52	0.85	6.84	1.63	4.49	0.72	5.16	0.78
M94-1-06	bd	46.10	2.74	0.03	0.08	0.02	0.28	0.88	0.64	3.86	0.92	6.90	1.59	4.71	0.81	5.62	0.78
M94-1-07	0.05	44.51	2.40	bd	0.03	0.01	0.26	0.74	0.63	3.49	0.85	6.60	1.62	4.62	0.76	4.81	0.78
M94-1-08	bd	43.20	2.22	0.01	0.03	0.01	0.24	0.62	0.48	3.08	0.79	6.69	1.53	4.47	0.66	4.55	0.73
M94-1-09	0.41	39.20	2.41	0.02	0.08	0.03	0.32	0.65	0.41	2.70	0.77	5.89	1.42	3.95	0.65	4.22	0.67
M94-1-10	bd	40.67	2.21	0.01	0.04	0.02	0.18	0.65	0.45	3.05	0.79	6.82	1.40	3.88	0.67	4.72	0.70
M94-1-11	bd	32.83	2.01	0.02	0.05	0.02	0.40	0.57	0.47	2.84	0.77	5.98	1.25	3.51	0.49	3.57	0.52
M94-1-12	0.13	44.65	8.43	0.03	0.07	0.02	0.34	1.40	0.76	3.74	0.91	6.90	1.55	4.49	0.74	4.97	0.84
M94-1-13	3.97	39.57	2.48	2.68	6.37	0.79	4.27	2.43	0.92	4.01	0.80	6.53	1.41	3.90	0.61	4.52	0.71
M94-1-14	bd	41.33	8.79	bd	0.02	0.02	0.43	0.91	0.55	3.54	0.78	6.92	1.53	4.22	0.62	4.14	0.77
M94-1-15	bd	48.41	10.79	0.01	0.05	0.01	0.36	1.56	0.79	4.48	1.06	7.90	1.90	4.96	0.74	5.63	0.85
M94-2-01	0.67	39.50	3.21	0.00	0.05	0.03	0.25	0.57	0.44	2.78	0.76	5.68	1.34	3.57	0.66	4.18	0.66
M94-2-02	bd	39.17	2.44	bd	0.06	0.04	0.48	0.47	0.35	2.10	0.70	5.45	1.45	4.20	0.64	4.09	0.66
M94-2-03	0.13	39.25	2.20	0.03	0.04	0.03	0.44	0.80	0.35	2.29	0.67	5.91	1.38	3.65	0.66	4.39	0.76
M94-2-04	0.38	41.45	2.25	0.00	0.06	0.03	0.29	0.39	0.43	2.90	0.81	6.08	1.42	3.94	0.73	4.59	0.70
M94-2-05	0.21	39.37	1.92	0.01	0.06	0.03	0.42	0.54	0.36	2.73	0.75	6.21	1.44	3.96	0.70	4.15	0.69
M94-2-06	5.34	40.55	2.82	0.03	0.07	0.02	0.29	0.65	0.43	3.05	0.86	6.51	1.45	4.13	0.62	4.71	0.69
M94-2-07	bd	39.21	1.98	0.02	0.05	0.03	0.52	0.65	0.33	2.10	0.71	6.06	1.44	4.08	0.65	4.26	0.74
M94-2-31r	0.29	44.76	8.74	0.06	0.21	0.05	0.45	1.17	0.60	3.72	0.94	7.71	1.53	5.02	0.78	5.29	0.80
M94-2-32r	0.35	45.15	11.03	0.03	0.17	0.04	0.41	1.18	0.68	3.81	0.92	7.60	1.65	4.93	0.86	4.93	0.76
M94-2-33c	0.06	49.69	9.77	0.02	0.10	0.01	0.27	1.44	0.83	3.98	0.98	7.90	2.02	5.44	0.90	5.73	0.89
M94-2-34c	0.02	50.17	8.10	0.00	0.05	0.02	0.27	1.44	0.81	3.74	1.06	8.12	2.01	5.78	0.87	6.01	0.91
M94-2-35m	0.13	47.14	10.55	0.05	0.10	0.02	0.34	1.31	0.71	3.60	0.94	7.28	1.84	4.83	0.79	5.20	0.91
M94-2-36m	bd	48.29	10.09	0.02	0.10	0.03	0.54	1.44	0.61	4.11	0.94	7.73	1.79	5.50	0.94	5.22	0.90
M94-5a-01	bd	43.62	4.21	0.01	0.03	0.02	0.33	1.04	0.58	3.26	0.89	6.72	1.64	5.08	0.75	4.71	0.80
M94-5a-02	bd	49.72	5.44	0.02	0.04	0.04	0.51	1.30	0.64	3.90	0.94	7.47	1.86	5.11	0.89	5.78	0.85
M94-5a-03	bd	46.16	4.35	bd	0.03	0.03	0.58	1.16	0.61	3.34	0.94	7.34	1.67	4.58	0.79	5.17	0.86
Omphacite																	
M94-1-20	7.53	1.31	14.31	0.60	2.58	0.46	2.26	0.89	0.25	0.76	0.12	0.50	0.05	0.07	0.01	0.06	0.00
M94-1-21	6.97	1.35	16.13	0.56	2.41	0.39	1.67	0.94	0.26	0.96	0.12	0.41	0.05	0.11	0.01	0.02	0.01
M94-5a-05	10.45	1.42	35.78	0.55	2.73	0.60	4.31	1.42	0.40	1.11	0.14	0.52	0.06	0.12	0.01	0.10	0.01
M94-5a-06	9.67	1.32	25.91	0.44	1.89	0.38	2.58	1.04	0.23	0.90	0.11	0.51	0.06	0.12	0.01	0.02	0.01

bd: Below detection limit.

omphacite are always above C1 chondrite values (Evensen et al., 1978). The clinopyroxene porphyroblasts have entirely different REE concentrations and patterns compared to those of omphacite. Clinopyroxenes are enriched in REE and keep a relative flat profile with a slight decrease (depilation) towards HREE (La_N 10.87–4.94, Yb_N 6.79–2.57) (Fig. 5a). Amphiboles in the retrograde symplectites and rims have slightly higher concentrations of REE (La_N 19.71–15.96, Yb_N 19.91–6.01) with respect to clinopyroxenes, but they have a similar HREE-depleted profile (Fig. 5b). Amphiboles have a slightly negative Eu anomaly (Eu_N 52.6–26.20) (Fig. 5b). Plagioclases contain very low REE contents with most values below the normalization values of C1 chondrites, and they show a LREE enrichment relative to HREE. Plagioclase has a sharp positive Eu anomaly (Eu_N 4.87–3.71) (Fig. 5c).

6. Thermodynamic modeling and *P–T* evolution

Understanding the *P–T* evolution of mafic rocks especially eclogites is complicated by the high variance and refractory nature of the mineralogy. Although it is difficult to estimate peak metamorphic pressures for the present assemblage using geobarometric estimates, the absence of plagioclase in the peak assemblage suggests that the assemblage must have equilibrated outside the plagioclase stability field, suggesting pressures above the plagioclase decomposition reaction suggested by Green and Ringwood (1967). To quantify this inference, phase relations for a bulk composition in the system $CaO–Na_2O–FeO–MgO–TiO_2–Al_2O_3–SiO_2–H_2O$, estimated from the mineral modes and compositions of a garnet + omphacite + clinopyroxene + rutile assemblage in a minor

amphibole–plagioclase-bearing domain, were computed as a function of pressure and temperature (Fig. 6) using free energy minimization (Connolly, 2005) with the thermodynamic data of Holland and Powell (1998); solution models are given in Table 5. The X_{Mg} [$Mg/(Fe+Mg)$] and X_{GrS} [$Ca/(Fe+Mg+Ca)$] isopleths for garnet and X_{Mg} and X_{Jd} [$Na/(Ca+Na)$] for clinopyroxene (Fig. 6) in the phase diagram section provide a basis for establishing the peak metamorphic conditions. The *P–T* conditions, at which the average composition of omphacite inclusions ($X_{Mg} = 0.76$, $X_{Jd} = 0.14$) preserved in the cores of garnets are predicted to be in equilibrium composition with the garnet cores ($X_{Mg} = 0.49$, $X_{GrS} = 0.19$), fall within the plagioclase-absent field for a clinopyroxene-garnet–rutile–melt at about 19–20 kbar and 1020 °C (Fig. 6). Thus we infer that the plagioclase-absent, garnet–omphacite–rutile assemblage must have equilibrated at a minimum pressure of 20 kbar and a temperature above 1020 °C (Fig. 6). The presence of rutile within the peak assemblage may reflect rutile exsolution from garnet during decompression. This effect cannot be reproduced in the phase equilibrium calculations because the garnet model does not account for Ti-solution, but the occurrence has been documented elsewhere. The absence of orthopyroxene in the studied samples and the presence of ilmenite-bearing symplectites together with the late amphibole rims and symplectites indicate a clear isothermal decompression and exhumation trajectory for the Sittampundi eclogites.

Recent studies from the PCSZ of high-pressure, ultrahigh-temperature granulites have reported contradictory *P–T* paths. Shimpo et al. (2006) suggested high-pressure, ultrahigh-temperature metamorphism from a garnet–corundum assemblage

Table 4
REE composition of clinopyroxene, amphibole and plagioclase determined by LA-ICPMS.

Sample	Sr	Y	Zr	La	Ce	Pr	Nd	Sm	Eu	Gd	Tb	Dy	Ho	Er	Tm	Yb	Lu
Clinopyroxene																	
M94-1-27	10.46	8.72	25.45	1.51	7.17	1.32	6.60	1.93	0.49	1.75	0.30	1.71	0.35	0.74	0.12	0.88	0.09
M94-1-28	12.06	10.62	23.99	1.77	8.40	1.47	7.48	2.27	0.61	2.28	0.36	2.45	0.45	1.01	0.16	0.83	0.13
M94-1-29	13.74	10.42	23.13	1.77	8.71	1.47	8.61	2.08	0.69	2.31	0.34	2.27	0.40	1.21	0.15	0.90	0.13
M94-1-30	8.90	6.51	19.69	1.39	6.12	1.15	5.43	1.89	0.50	1.67	0.27	1.52	0.28	0.73	0.13	0.59	0.08
M94-1-31	9.87	8.08	21.49	1.55	7.30	1.33	6.32	1.67	0.50	1.52	0.26	1.71	0.32	0.68	0.11	0.86	0.09
M94-2-13	14.54	10.69	21.98	1.96	9.84	2.22	11.73	3.29	1.02	2.76	0.38	2.08	0.40	1.04	0.12	0.99	0.14
M94-2-14	11.16	9.59	27.13	1.69	8.48	1.91	11.38	3.25	0.84	2.68	0.36	2.13	0.33	0.93	0.13	0.75	0.11
M94-2-15	12.75	10.09	26.92	1.73	8.66	1.94	11.56	3.32	0.99	2.98	0.39	2.39	0.39	0.89	0.14	0.84	0.09
M94-2-16	11.40	8.38	25.48	1.51	8.08	1.75	9.22	2.54	0.77	2.16	0.32	1.76	0.33	0.75	0.10	0.72	0.08
M94-2-17	8.93	6.04	26.97	1.56	7.32	1.40	7.43	1.97	0.53	1.83	0.25	1.47	0.28	0.66	0.10	0.58	0.11
M94-2-18	9.00	5.76	27.43	1.55	6.86	1.38	6.81	1.74	0.54	1.67	0.25	1.27	0.23	0.60	0.07	0.41	0.10
M94-2-19	9.21	5.10	23.79	1.47	6.42	1.27	6.09	1.82	0.51	1.50	0.23	1.26	0.21	0.54	0.06	0.37	0.10
M94-2-21	13.16	7.23	22.37	1.63	6.43	1.22	6.61	1.73	0.49	1.82	0.26	1.50	0.26	0.69	0.09	0.53	0.09
M94-2-22	11.78	9.13	17.42	1.42	6.73	1.39	7.20	2.64	0.56	2.23	0.39	2.04	0.42	0.88	0.14	0.65	0.12
M94-2-23	10.70	8.86	23.29	1.53	7.87	1.55	8.72	2.48	0.75	2.31	0.35	1.83	0.38	0.84	0.14	0.69	0.12
M94-2-24	7.94	8.55	22.31	1.36	7.04	1.55	9.00	2.80	0.76	2.64	0.32	1.99	0.35	0.85	0.10	0.77	0.10
M94-2-25	21.09	17.47	24.91	2.47	12.83	2.91	16.65	5.37	1.52	5.13	0.66	3.99	0.75	1.69	0.24	1.22	0.20
M94-2-26	20.27	13.61	21.70	2.31	10.61	2.24	12.22	3.38	0.98	3.14	0.52	3.27	0.61	1.54	0.20	1.01	0.15
M94-2-27	26.66	14.06	24.83	2.66	12.84	2.67	14.27	4.35	1.26	4.05	0.55	2.95	0.58	1.25	0.18	1.12	0.20
M94-2-28	20.02	12.52	21.53	2.25	11.07	2.29	13.46	3.72	1.05	3.57	0.49	2.62	0.50	1.17	0.18	1.23	0.15
M94-2-29	19.69	12.28	20.96	2.17	10.65	2.23	12.31	3.51	0.99	3.11	0.47	2.64	0.47	1.12	0.15	0.94	0.18
M94-2-30	13.94	8.73	19.72	1.66	7.88	1.69	8.85	2.50	0.78	2.57	0.32	1.90	0.33	0.70	0.12	0.65	0.12
M94-5a-07	11.28	8.19	19.62	1.50	6.93	1.17	5.74	1.81	0.55	1.56	0.31	1.53	0.34	0.74	0.10	0.77	0.08
M94-5a-08	8.25	6.05	19.13	1.21	5.13	0.92	4.76	1.29	0.39	1.39	0.23	1.07	0.24	0.59	0.08	0.42	0.06
Amphibole																	
M94-1-22	35.29	24.48	31.26	3.91	17.38	3.14	16.54	4.78	1.52	5.34	0.92	5.53	1.23	2.42	0.22	0.99	0.13
M94-1-23	39.01	30.87	42.58	4.78	21.77	3.96	21.33	5.60	1.97	5.51	1.05	6.45	1.17	2.62	0.44	1.84	0.16
M94-1-24	36.94	28.88	39.29	4.83	21.81	3.75	21.12	5.76	1.87	5.40	1.03	6.10	1.13	2.46	0.42	2.04	0.31
M94-1-25	32.55	22.33	32.58	3.98	18.34	3.22	16.32	4.70	1.42	4.96	0.78	4.48	0.86	2.03	0.31	1.85	0.28
M94-1-26	69.27	26.99	30.05	4.22	17.67	3.39	17.62	6.09	1.74	5.45	0.85	5.54	1.04	2.47	0.37	2.33	0.27
M94-2-10	48.26	44.66	32.51	4.70	23.10	5.53	33.12	10.57	3.02	13.14	1.76	10.07	1.68	3.87	0.60	2.85	0.51
M94-2-12	60.99	43.15	24.56	4.11	22.35	4.93	29.96	9.94	2.46	10.19	1.63	8.69	1.54	3.24	0.55	3.29	0.39
M94-2-37	45.51	26.47	35.06	4.04	19.14	3.72	17.75	4.61	1.86	5.66	0.78	4.97	1.03	2.38	0.40	2.45	0.36
M94-2-38	45.77	36.73	37.76	4.67	23.86	4.98	27.04	7.64	2.32	7.79	1.37	7.81	1.39	3.63	0.46	3.11	0.34
Plagioclase																	
M94-1-16	279.32	0.10	0.05	0.78	1.04	0.09	0.30	bd	0.27	bd	0.01	0.06	0.01	0.02	0.00	0.02	bd
M94-1-17	267.14	0.30	0.12	0.70	0.97	0.07	0.18	0.04	0.22	0.04	0.00	0.05	0.01	0.04	0.00	0.03	0.00
M94-1-18	292.44	0.08	0.01	0.78	1.16	0.06	0.28	0.06	0.20	0.01	0.00	0.04	0.01	0.00	0.01	0.01	0.00
M94-1-19	302.60	0.11	0.21	0.80	1.06	0.09	0.31	0.03	0.28	0.02	0.00	0.02	0.00	0.01	0.00	0.02	bd

from nearby localities. This conclusion was based on the occurrence of porphyroblastic garnet + corundum and the presence of Mg-rich staurolite (X_{Mg} up to 0.51) and kyanite in garnet. From this observation the authors inferred a probable eclogite facies condition followed by continuous heating to ultrahigh-temperature (T 940–990 °C) through a clockwise trajectory based on consideration of the quartz-absent MgO–Al₂O₃–SiO₂ petrogenetic grid. Kelsey et al. (2006) pointed out that the conclusions of Shimpo et al. (2006) were based on a MgO–Al₂O₃–SiO₂ model chemical system that is inappropriate for these Fe-rich rocks and consequently they gave rise to an overestimate of the metamorphic pressures. Kelsey et al. (2006) also argued that the assemblage garnet–corundum can be stable at relatively low P – T conditions. In the response to Kelsey et

al. (2006), Tsunogae and Santosh (2006) observed that the textural evidence provided by Shimpo et al. (2006) is unique and indicative of a high-pressure condition. Santosh and Sajeev (2006) reported garnet-absent corundum and sapphirine-bearing hyper-aluminous Mg-rich and silica-poor ultrahigh-temperature granulites from a number of localities within the PCSZ from which they constructed a tight 'hairpin-type' anticlockwise P – T trajectory. Finally, Collins et al. (2007) reported an isothermal decompression profile for garnet-bearing ultrahigh-temperature granulites in the PCSZ.

Considering the above contradictory interpretations it is important for us to assess the mode of the prograde P – T segment of the Sittampundi eclogites, which is situated only a few kilometres northwest of the above locations. However, it is difficult to

Table 5
Solution notation, formulae and model sources for phase diagram calculation.

Symbol	Solution	Formula	Source
Cpx	Clinopyroxene	Na _{1-y} Ca _{2y} Mg _{xy} Fe _{(1-x)y} Al _y Si ₂ O ₆	1
Grt	Garnet	Fe _{3x} Ca _{3y} Mg _{3(1-x+y+z/3)}} Al _{2-2z} Si _{3+z} O ₁₂ , $x+y \leq 1$	2
Opx	Orthopyroxene	[Mg _x Fe _{1-x}] _{4-2y} Al _{4(1-y)}} Si ₄ O ₁₂	1
Melt	Melt	Na–Mg–Al–Si–K–Ca–Fe hydrous silicate melt	3, 4
Amph	Amphibole	Ca _{2-2w} Na _{z+2w} [Mg _x Fe _{1-x}] _{3+2y+z} Al _{3-3y-w} Si _{7+w+y} O ₂₂ (OH) ₂ , $w+y+z \leq 1$	5
Pl	Feldspar	K _y Na _x Ca _{1-x-y} Al _{2-x-y} Si _{2+x+y} O ₈ , $x+y \leq 1$	6

Unless otherwise noted, the compositional variables x , y , and z may vary between zero and unity and are determined as a function of the computational variables by free-energy minimization.

Sources: 1—Holland and Powell (1996); 2—Holland and Powell (1998); 3—Holland and Powell (2001); 4—White et al. (2001); 5—Dale et al. (2005); 6—Führman and Lindsley (1988).

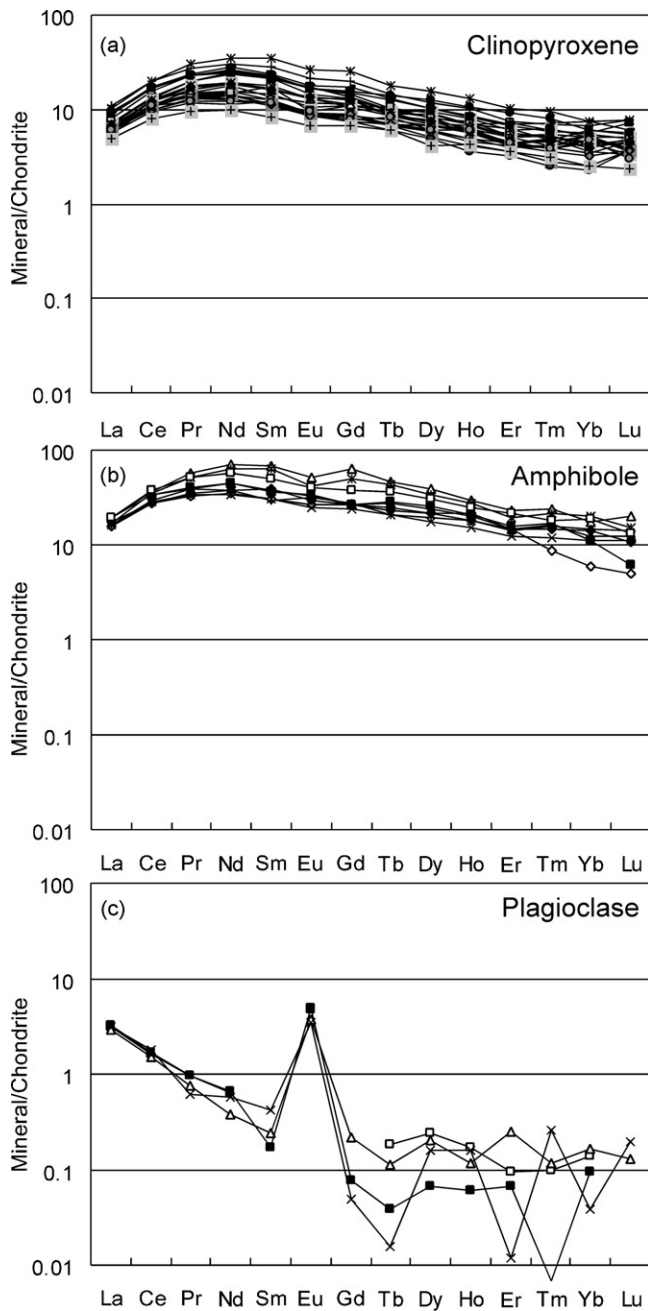


Fig. 5. C1 chondrite-normalized REE pattern of clinopyroxene (a) and retrograde minerals, amphibole (b) and plagioclase (c) from Sittampundi eclogite. See text for further discussion.

find evidence for the prograde evolution in mafic granulites and eclogites. Apart from omphacite and rutile exsolution, the only early phase in the Sittampundi eclogites is ilmenite occurring as inclusions in garnet, but it does provide useful evidence for defining a possible prograde path. Based on our P – T phase diagram sections, ilmenite is only stable at a pressure below 11 kbar. In the absence of orthopyroxene or amphibole inclusions in garnet, the presence of ilmenite suggests that a prograde evolution from an ilmenite-stable orthopyroxene/amphibole-absent field to an ilmenite–orthopyroxene–amphibole-absent state. Fig. 6 indicates that the prograde segment must be on the high-temperature side of the retrograde P – T path. This suggests that the P – T trajectory of the Sittampundi eclogites was possibly a tight anticlockwise ‘hairpin-type’, similar to that reported by Santosh and Sajeev (2006).

7. Tectonic scenario: a discussion

Many authors have introduced novel classifications, concepts and hypotheses to explain the origin of eclogites. Most commonly accepted is the group A, B and C classification of Coleman et al. (1965). Group A includes low-Jd, clinopyroxene-bearing, Cr-rich eclogites in high-magnesium whole-rocks. Group B eclogites contain a moderate Jd component in LREE-depleted clinopyroxenes, and garnets that are extremely LREE-depleted and HREE-enriched. Group C eclogites are Jd-rich and contain grossular-rich garnets and a significant positive Eu in primary minerals. Also there are two main genetic models for the genesis of eclogites. First is the ‘crustal hypothesis’ (e.g., Taylor and Neal, 1989; Ireland et al., 1994), according to which eclogites are the exhumed remnants of subducted oceanic crust that may or may not have undergone partial melting. A variable of the crustal hypothesis concerns the metamorphism and isobaric cooling of mafic lower crust (e.g., Griffin et al., 1990; Pearson et al., 1991), or the partial melting of subducted oceanic crust (e.g., Barth et al., 2001). Second is the ‘mantle hypothesis’, which suggests high-pressure (about 30 kbar at ca. 100 km depth) crystallization of eclogite from a peridotitic magma that has ascended through the lithosphere (e.g., Caporuscio and Smyth, 1990).

The Sittampundi eclogites are relatively low-magnesium and contain moderate Jd-bearing omphacitic clinopyroxenes that show a slight depletion in LREE, and garnets that are extremely depleted in LREE and generally enriched in HREE that have a flat profile. These compositional features point towards group B eclogites with a crustal provenance. The whole-rock chemistry recalculated from the model percentage of the minerals indicates about ca. 10 wt% MgO, ca. 48 wt% SiO₂ and ca. 15 wt% CaO. This composition is very similar to that of Archaean basalts and low-MgO eclogites reported from West Africa (Barth et al., 2001). Mantle-derived eclogites generated by the melting and metastability of olivine due to the expansion of stable garnet and Jd-rich clinopyroxene produce a picritic melt with a high magnesium and low aluminium content. The fact that the Sittampundi eclogites have a low magnesian composition, a metamorphic pressure (ca. 20 kbar) lower than that of mantle-derived eclogite (above 30 kbar), and a composition similar to that of Archaean basalt suggests that the protolith was close to a basaltic composition.

The ultrahigh-temperature (>1000 °C) and high-pressure (20 kbar) eclogites in the Sittampundi complex confirm the concept that the Palghat–Cauvery shear zone system represents a major suture zone between Archaean crustal blocks to the north and the Madurai block to the south; in fact the eclogites provide the best petrochemical and viable evidence adduced so far that supports a suture zone. If the general southerly dip of rocks in the suture zone suggests that subduction was towards the south, this would mean that the older block to the north was in the footwall, and the younger southerly block in the hanging wall.

In spite of uncertainties about the origin of some rocks in the PCSZ, we know that Sittampundi is an Archaean layered igneous complex (Bhaskar Rao et al., 1996) that was subducted to pressure > 20 kbar (ca. 65 km paleo-depth) at a temperature > 1000 °C, and that the subduction–exhumation gave rise to a ‘hairpin-type’ anticlockwise P – T trajectory, probably in the latest Neoproterozoic–Cambrian. This took place when these rocks were at the leading edge of the Archaean Dharwar crustal block that was involved in subduction–collision tectonics during the final assembly of East Gondwana (Yoshida et al., 2003; Santosh and Sajeev, 2006). A key feature of wedge extrusion in a subduction zone is the development of an isoclinal anticline in the centre of the exhumed wedge (Maruyama et al., 1996; Maruyama, 1997; Kawai et al., 2007). The Sittampundi complex is folded into an isoclinal anticline with characteristics that preclude it being a ‘normal’ regional tectonic

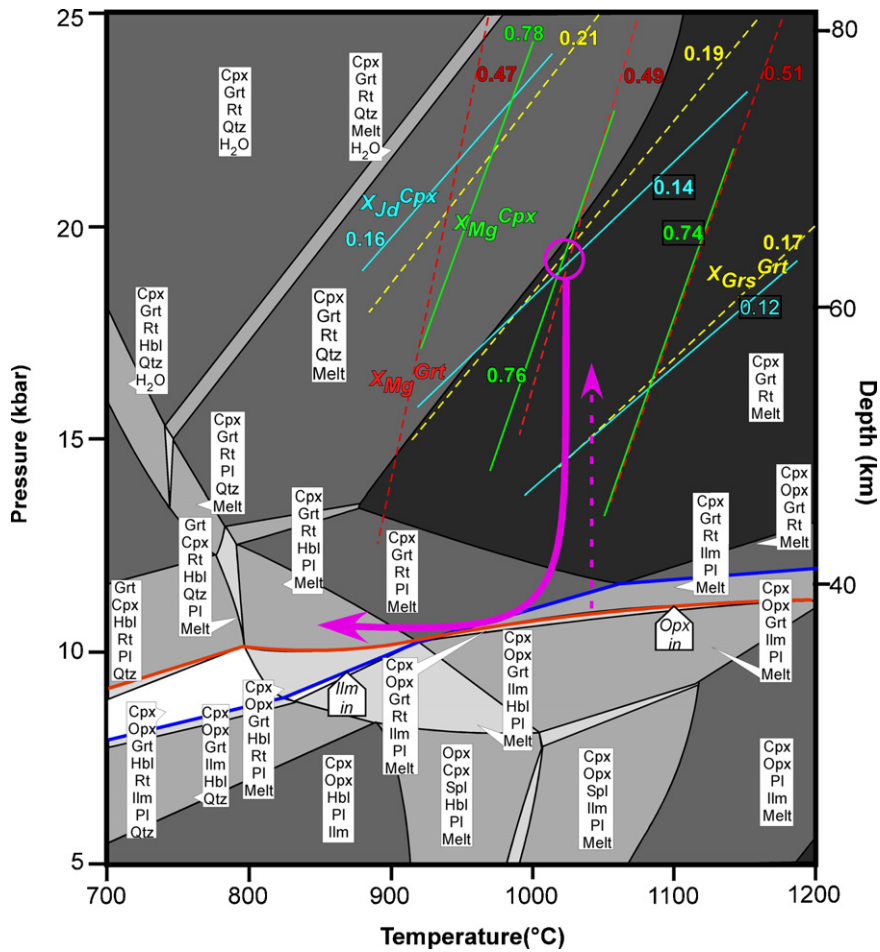


Fig. 6. A P - T phase diagram section modeled in the $\text{CaO-Na}_2\text{O-FeO-MgO-TiO}_2\text{-Al}_2\text{O}_3\text{-SiO}_2\text{-H}_2\text{O}$ system calculated for the bulk chemical composition 15.13:1.46:11.00:10.14:0.39:13.44:47.93:0.51 for partly retrogressed Sittampundi eclogite. The open circle represents the peak metamorphic condition derived from the compositional isopleths. The solid arrow line marks the retrograde P - T segment, while the dashed arrow represents the possible prograde path.

fold. There are no significant minor folds associated with the major anticline, and the limbs have undergone extreme thinning over tens of kilometres but not in relation to any specific fold-limb attenuation. The layered complex and its isoclinal fold predate the emplacement of the protoliths of the TTG orthogneisses, which were not deformed by comparable isoclinal folds. We suggest that the Sittampundi complex is an exhumation isoclinal anticline of high-pressure rocks that were emplaced upwards in the subduction zone and are now located near the centre of the subduction complex of the PCSZ.

Some segments of Phanerozoic orogenic belts, like the Qinling and Dabie Shan in China (Yang et al., 2003), South Korea (Kwon et al., 2009) and West Norway (Kylander-Clark et al., 2007) comprise amphibolite facies gneisses that contain only a few percent of eclogitic lenses (just like the PCSZ) and amphibolite facies gneisses in the ca. 1.0 Ga Glenelg-Attadale inlier in Scotland contain about 25% of eclogite lenses (Brewer et al., 2003). While the eclogites have retained evidence of their subduction to high-pressure, their host gneisses have retrogressed from their eclogite facies assemblages, through the granulite facies, to their present amphibolite facies state. For example, in western Norway amphibolite facies gneisses that occupy an area ca. 60,000 km² contain only a few volume percent of eclogite lenses, and yet it is widely accepted today that the gneisses were likewise subducted to eclogite facies depths (Kylander-Clark et al., 2007).

Textural data from many high-grade basement terranes reveal that usually the basic lithologies lag behind the gneisses in their

retrogression, and so retain their granulite facies mineralogy, while ultramafic rocks retain not only their granulite facies minerals, but even vestiges of their original high-pressure assemblages. Water was the agent responsible for the retrogression; it appears to have flushed through the pervasively gneisses easily, while the mafic and ultramafic rocks remained impermeable.

From our fieldwork we know that eclogites occur in several parts of the PCSZ and therefore we are led to the conclusion that many parts of it have been subducted to high- P depths and later exhumed to a mid-crustal level, where the host gneisses were hydrated and re-equilibrated to their present amphibolite facies state. Most of the P - T trajectories so far published from the PCSZ only record the post-peak exhumation history of the rocks. Future research may be able to define other areas of the suture zone that have undergone high-pressure metamorphism and better constrain the pre-peak P - T trajectory.

Acknowledgements

We acknowledge constructive comments from M. Santosh and T. Tsunogae. We also thank Peter Cawood for the editorial handling. We are grateful to T. Itaya, T. Hirata, S. Maruyama, S. Kwon and M. Santosh for facilities and encouragement. KS acknowledges a Grant-in-aid for JSPS Fellows (Krishnan Sajeev, No: P05066). This work was also supported by the second stage of Brain Korea (BK) 21 Project.

References

- Barth, M.G., Rudnick, R.L., Horn, I., McDonough, W.F., Spicuzza, M.J., Valley, J.W., Haggerty, S.E., 2001. Geochemistry of xenolithic eclogites from West Africa, Part I: a link between low MgO eclogites and Archean crust formation. *Geochimica et Cosmochimica Acta* 65, 1499–1527.
- Bartlett, J.M., Dougherty-Page, J.S., Harris, N.B.W., Hawkesworth, C.J., Santosh, M., 1998. The application of single zircon evaporation and model Nd ages to the interpretation of polymetamorphic terrains: an example from the Proterozoic mobile belt of South India. *Contributions to Mineralogy and Petrology* 131, 181–195.
- Bhaskar Rao, Y.J., Chetty, T.R.K., Janardhan, A.S., Gopalan, K., 1996. Sm–Nd and Rb–Sr ages and *P–T* history of the Archean Sittampundi and Bhavani layered meta-anorthositic complexes in Cauvery shear zone, South India: evidence for Neoproterozoic reworking of Archean crust. *Contributions to Mineralogy and Petrology* 125, 237–250.
- Bhaskar Rao, Y.J., Janardhan, A.S., Vijaya Kumar, T., Narayana, B.L., Dayal, A.M., Taylor, P.N., Chetty, T.R.K., 2003. Sm–Nd model ages and Rb–Sr isotope systematics of charnockites and gneisses across the Cauvery shear zone, southern India: implications for the Archaean–Neoproterozoic boundary in the southern granulite terrain. In: Ramakrishnan, M. (Ed.), *Tectonics of Southern Granulite Terrain*, vol. 50. Geological Society India Memoir, pp. 297–317.
- Brewer, T.S., Storey, C.D., Parrish, R.R., Temperley, S., Windley, B.F., 2003. Grenvillian age decompression of eclogites in the Glenelg–Attadale inlier, NW Scotland. *Journal of Geological Society, London* 160, 565–674.
- Caporuscio, F.A., Smyth, J.R., 1990. Trace element crystal chemistry of mantle eclogites. *Contributions to Mineralogy and Petrology* 105, 550–561.
- Chappel, B.W., White, A.J.R., 1970. Further data on an eclogite from Sittampundi complex, India. *Mineralogical Magazine* 37, 555–560.
- Chetty, T.R.K., 1996. Proterozoic shear zones in southern granulite terrain, India. In: Santosh, M., Yoshida, M. (Eds.), *The Archaean and Proterozoic Terrains in southern India within East Gondwana*, vol. 3. Gondwana Research Group Memoir, pp. 77–89.
- Chetty, T.R.K., Bhaskar Rao, Y.J., 2006. The Cauvery shear zone, Southern Granulite Terrain, India: a crustal-scale flower structure. *Gondwana Research* 10, 77–85.
- Coleman, R.G., Lee, D.E., Beatty, L.B., Brannock, W.W., 1965. Eclogites and eclogites: their differences and similarities. *Geological Society of America Bulletin* 76, 483–508.
- Collins, A.S., 2006. Madagascar and the amalgamation of Central Gondwana. *Gondwana Research* 9, 3–16.
- Collins, A.S., Windley, B.F., 2002. The tectonic evolution of central and northern Madagascar and its place in the final assembly of Gondwana. *Journal of Geology* 110, 325–340.
- Collins, A.S., Clark, C., Sajeev, K., Santosh, M., Kelsey, D.E., Hand, M., 2007. Passage through India: the Mozambique Ocean suture, high pressure granulites and the Palghat–Cauvery shear zone system. *Terra Nova* 19, 141–147.
- Connolly, J.A.D., 2005. Computation of phase equilibria by linear programming: a tool for geodynamic modeling and its application to subduction zone decarbonation. *Earth and Planetary Science Letters* 236, 524–541.
- Dale, J., Powell, R., White, R.W., Elmer, F.L., Holland, T.J.B., 2005. A thermodynamic model for Ca–Na clinopyroxenes in Na₂O–CaO–FeO–MgO–Al₂O₃–SiO₂–H₂O for petrological calculations. *Journal of Metamorphic Geology* 23, 771–791.
- Deters-Umlauf, P., Srikantappa, C., Köhler, h., 1998. Pan-African ages in the Moyar and Bhavani shear zones (South India). *Indian Mineralogist* 32, 123–124.
- Drury, S.A., Holt, R.W., 1980. The tectonic framework of the South Indian craton: a reconnaissance involving LANDSAT imagery. *Tectonophysics* 65, 1–15.
- Evensen, N.M., Matthey, D.P., O’Nions, R.K., 1978. Rare earth abundances in chondritic meteorites. *Geochimica et Cosmochimica Acta* 42, 1199–1212.
- Fuhrman, M.L., Lindsley, D.H., 1988. Ternary-Feldspar Modeling and Thermometry. *American Mineralogist* 73, 201–215.
- Geological Survey of India, 1995. 1: 500,000 Geological and mineral map of Tamil Nadu and Pondicherry, Madras.
- Ghosh, J.G., de Wit, M.J., Zartman, R.E., 2004. Age and tectonic evolution of Neoproterozoic ductile shear zones in the Southern Granulite Terrain of India, with implications for Gondwana studies. *Tectonics* 23 (TC3006), doi:10.1029/2002TC001444.
- Green, D.H., Ringwood, A.E., 1967. An experimental investigation of the gabbro to eclogite transformation and its petrological applications. *Geochimica et Cosmochimica Acta* 31, 767–833.
- Griffin, W.L., Jensen, B.B., Misra, S.N., 1971. Anomalous elongated rutile in eclogite-facies pyroxene and garnet. *Norsk Geologisk Tidsskrift* 51, 177–185.
- Griffin, W.L., O’Reilly, S.Y., Pearson, N.J., 1990. Eclogite stability near the crust–mantle boundary. In: Carswell, D.A. (Ed.), *Eclogite Facies Rocks*. Blackie, Glasgow and London, pp. 291–314.
- Harinarayana, T., Naganjaneyulu, K., Patro, B.P.K., 2006. Detection of a collision zone in South Indian shield region from magnetotelluric studies. *Gondwana Research* 10, 48–56.
- Harris, N.B.W., Bartlett, J.M., Santosh, M., 1996. Neodymium isotope constraints on the tectonic evolution of East Gondwana. *Journal of Southeast Asian Earth Science* 14, 119–125.
- Harris, N.B.W., Santosh, M., Taylor, P.N., 1994. Crustal evolution in South India: constraints from Nd isotopes. *Journal of Geology* 102, 139–150.
- Holland, T.J.B., Powell, R., 1996. Thermodynamics of order–disorder in minerals. 2. Symmetric formalism applied to solid solutions. *American Mineralogist* 81, 1425–1437.
- Holland, T.J.B., Powell, R., 1998. An internally consistent thermodynamic data set for phases of petrological interest. *Journal of Metamorphic Geology* 16, 309–343.
- Holland, T.J.B., Powell, R., 2001. Calculation of phase relations involving haplogranitic melts using an internally consistent thermodynamic dataset. *Journal of Petrology* 42, 673–683.
- Iizuka, T., Hirata, T., 2004. Simultaneous determinations of U–Pb age and REE abundances for zircons using ArF excimer laser ablation–ICPMS. *Geochemical Journal* 38, 229–241.
- Ireland, T.R., Rudnick, R.L., Spetsius, Z., 1994. Trace elements in diamond inclusions from eclogites reveal link to Archean granites. *Earth and Planetary Science Letters* 128, 199–213.
- Janardhanan, A.S., Leake, B.E., 1974. Sapphirine in Sittampundi complex, India. *Mineralogical Magazine* 39, 901–902.
- Janardhanan, A.S., Leake, B.E., 1975. The origin of the meta-anorthositic gabbros and garnetiferous granulites of the Sittampundi complex, Madras, India. *Journal of Geological Society of India* 16, 391–408.
- Katayama, I., Parkinson, C.D., Okamoto, K., Nakajima, Y., Maruyama, S., 2002. Super-silicic clinopyroxene and silica exsolution in UHP rocks from the Kokchetav Massif. In: Parkinson, C.D., Katayama, I., Liou, J.G., Maruyama, S. (Eds.), *Diamond-Bearing Kokchetav Massif*, vol. 35. Universal Academy Press, Frontiers Science Series, Kazakhstan, pp. 157–165.
- Kawai, T., Windley, B.F., Terabayashi, M., Yamamoto, H., Maruyama, S., Omori, S., Shibuya, T., Sawaki, Y., Isozaki, Y., 2007. Geotectonic framework of the blueschist unit on Anglesey–Llwyn, UK, and its role in the development of a Neoproterozoic accretionary orogen. *Precambrian Research* 153, 11–28.
- Kelsey, D.E., Clark, C., Hand, M., Collins, A.S., 2006. Comment on “First report of garnet–corundum rocks from southern India: implications for prograde high-pressure (eclogite-facies?) metamorphism”. *Earth and Planetary Science Letters* 249, 529–534.
- Kwon, S., Sajeev, K., Mitra, G., Park, Y., Kim, S.W., 2009. Evidence of Permo-Triassic collision in Far East Asia: the Korean collisional orogen. *Earth and Planetary Science Letters*, doi:10.1016/j.epsl.2009.01.016.
- Kylander-Clark, A.R.C., Hacker, B.R., Johnson, C.M., Beard, B.L., Mahlen, N.J., Lapen, T.J., 2007. Coupled Lu–Hf and Sm–Nd geochronology constrains prograde exhumation histories of high- and ultrahigh-pressure eclogites from western Norway. *Chemical Geology* 242, 137–154.
- Leake, B.E., Janardhanan, A.S., Kemp, A., 1976. High P H₂O and hornblende in the Sittampundi complex, India. *Mineralogical Magazine* 40, 525–526.
- Maruyama, S., 1997. Pacific-type orogeny revisited: Miyashiro-type orogeny proposed. *The Island Arc* 6, 91–120.
- Maruyama, S., Liou, J.G., Terabayashi, M., 1996. Blueschists and eclogites of the world and their exhumation. *International Geology Review* 38, 485–594.
- Maruyama, S., Okamoto, K., 2007. Water transportation from the subducting slab into the mantle transition zone. *Gondwana Research* 11, 148–165.
- Meißner, B., Deters, P., Srikantappa, C., Köhler, H., 2002. Geochronological evolution of the Moyar, Bhavani and Palghat shear zones of southern India: implications for East Gondwana correlations. *Precambrian Research* 114, 149–175.
- Meert, J.G., 2003. A synopsis of events related to the assembly of eastern Gondwana. *Tectonophysics* 362, 1–40.
- Meert, J.G., Lieberman, B.S., 2008. The Neoproterozoic assembly of Gondwana and its relationship to the Ediacaran–Cambrian radiation. *Gondwana Research* 14, 5–21.
- Nishimiya, Y., Tsunogae, T., Santosh, M., 2008. Petrology and fluid inclusions of garnet–clinopyroxene rocks from Paramati in the Palghat–Cauvery shear zone system, southern India. *Journal of Mineralogical and Petrological Sciences* 103, 354–360.
- Pearson, N.J., O’Reilly, S.Y., Griffin, W.L., 1991. The granulite to eclogite transition beneath the eastern margin of the Australian craton. *European Journal of Mineralogy* 3, 293–322.
- Ramadurai, S., Sankaran, M., Selvan, T.A., Windley, B.F., 1975. The stratigraphy and structure of the Sittampundi complex, Tamil Nadu. *Journal of Geological Society of India* 16, 409–414.
- Rao, V.V., Prasad, B.R., 2006. Structure and evolution of the Cauvery shear zone system, Southern Granulite Terrain, India: evidence from deep seismic and other geophysical studies. *Gondwana Research* 10, 29–40.
- Rino, S., Kon, Y., Sato, W., Maruyama, S., Santosh, M., Zhao, D., 2008. The Grenvillian and Pan-African orogens: world’s largest orogenies through geologic time, and their implications on the origin of superplume. *Gondwana Research* 14, 51–72.
- Robinson, P., Spear, F.S., Schumacher, J.C., Laird, J., Klein, C., Evans, B.W., Doolan, B.L., 1982. Phase relations of metamorphic amphiboles: natural occurrence and theory. In: Veblen, D.R., Ribbe, P.H. (Eds.), *Amphiboles: Petrology and Experimental Phase Relations*, vol. 9B. Mineralogical Society of America, pp. 1–227.
- Santosh, M., Sajeev, K., 2006. Anticlockwise evolution of ultrahigh-temperature granulites within continental collision zone in southern India. *Lithos* 92, 447–464.
- Santosh, M., Tsunogae, T., Koshimoto, S., 2004. First report of sapphirine-bearing rocks from the Palghat–Cauvery shear zone system, southern India. *Gondwana Research* 7, 620–626.
- Santosh, M., Collins, A.S., Tamashiro, I., Koshimoto, S., Tsutsumi, Y., Yokoyama, K., 2006. The timing of ultrahigh-temperature metamorphism in southern India: U–Th–Pb electron microprobe ages from zircon and monazite in sapphirine-bearing granulites. *Gondwana Research* 10, 128–155.
- Shimpo, M., Tsunogae, T., Santosh, M., 2006. First report of garnet–corundum rocks from southern India: implications for prograde high-pressure (eclogite-facies?) metamorphism. *Earth and Planetary Science Letters* 242, 111–129.

- Subramaniam, A.P., 1956. Mineralogy and petrology of the Sittampundi complex, Salem district, Madras State, India. *Geological Society of America Bulletin* 67, 317–390.
- Taylor, L.A., Neal, C.R., 1989. Eclogites with oceanic crustal and mantle signatures from the Bellsbank kimberlite, South Africa, Part I: mineralogy, petrography, and whole rock chemistry. *Journal of Geology* 97, 551–567.
- Tsunogae, T., Santosh, M., 2005. Ti-free h ogbomite in spinel- and sapphirine-bearing Mg–Al rock from the Palghat–Cauvery shear zone system, southern India. *Mineralogical Magazine* 69, 937–949.
- Tsunogae, T., Santosh, M., 2006. In: Kelsey, D.E., Clark, C., Hand, M., Collins, A.S. (Eds.), Reply to Comment on “First report of garnet–corundum rocks from southern India: implications for prograde high–pressure (eclogite-facies?) metamorphism”, vol. 249. *Earth and Planetary Science Letters*, pp. 535–540.
- White, R.W., Powell, R., Holland, T.J.B., 2001. Calculation of partial melting equilibria in the system Na₂O–CaO–K₂O–FeO–MgO–Al₂O₃–SiO₂–H₂O (NCKFMASH). *Journal of Metamorphic Geology* 19, 139–153.
- Windley, B.F., Selvan, T.A., 1975. Anorthosites and associated rocks of Tamil Nadu, southern India. *Journal of Geological Society of India* 16, 209–215.
- Windley, B.F., Bishop, F.C., Smith, J.V., 1981. Metamorphosed layered igneous complexes in Archean granulite–gneiss belts. *Annual Review of Earth and Planetary Science* 9, 175–198.
- Yang, J.S., Xu, Z.Q., Dobrzhinetskaya, L.F., Green, H.W., Pei, X., Shi, R., Wu, C., et al., 2003. Discovery of metamorphic diamonds in central China: an indication of a 14,000-km-long zone of deep subduction resulting from multiple continental collisions. *Terra Nova* 15, 370–379.
- Yoshida, M., Jacobs, J., Santosh, M., Rajesh, H.M., 2003. Role of Pan-African events in the circum-east Antarctic orogen of East Gondwana: a critical review. In: Yoshida, M., Windley, B.F., Dasgupta, S. (Eds.), *Proterozoic East Gondwana: Supercontinent Assembly and Breakup*, vol. 206. Geological Society of London Special Publication, pp. 57–75.